Taylor & Francis
Taylor & Francis Group

Numerical Heat Transfer, Part B: Fundamentals

An International Journal of Computation and Methodology

ISSN: (Print) (Online) Journal homepage: https://www.tandfonline.com/loi/unhb20

Thermal radiation effect on the Maxwell graphene based nanofluid passing through a squeezing channel

Rohit Sharma, Manoj Kumar Mishra, Kuracha Nirisha, Vatukuru Nagaradhika & Ali J. Chamkha

NUMERICAL HEAT TRANSFER, PART B: FUNDAMENTALS
https://doi.org/10.1080/10407790.2023.2279088

Thermal radiation effect on the Maxwell graphene based nanofluid passing through a squeezing channel

Rohit Sharma[a], Manoj Kumar Mishra[b], Kuracha Nirisha[a], Vatukuru Nagaradhika[a], and Ali J. Chamkha[c]

[a]Department of Mathematics, School of Sciences, GITAM (Deemed to be University), Bengaluru, India; [b]Department of Mathematics, School of Advanced Sciences, VIT-AP University, Amaravati, India; [c]Faculty of Engineering, Kuwait College of Science and Technology, Doha District

ABSTRACT

This article presents a comparative analysis of flow and heat transfer characteristics of magnetohydrodynamic flow of non-Newtonian base fluid (ethylene glycol) and nanofluid (ethylene glycol + graphene) between two parallel plates moving toward/apart to each other. The study also includes the effects of Joule dissipation, thermal radiation, and heat absorption. The mathematical model that governs the flow of the above-described problem is a single-phase flow model for nanofluids that is augmented with the non-Newtonian Maxwell fluid model. Similarity transformation was used to change controlling partial differential equations into coupled non-dimensional ordinary differential equations. The numerical solution is obtained by employing the shooting technique along with fourth order Runge–Kutta Fehlberg method. The impact of several physical characteristics on fluid velocity, temperature, the coefficient of skin friction, and the heat transfer rate is also explored. As a result, this research has the potential to be used in biomedical engineering as well as powder technology.

ARTICLE HISTORY
Received 9 June 2023
Revised 11 October 2023
Accepted 27 October 2023

KEYWORDS
Absorption; Joule dissipation; Maxwell fluid; MHD; nanofluid

1. Introduction

Nanofluids have been a major consideration nowadays due to their amazing properties in industry and public endeavor. Masuda et al. [1] pioneered the idea of nanofluid by demonstrating an enhanced thermal conductivity in colloidal suspension of water γ-Al_2O_3. Later in 1995, Choi [2] first used the term nanofluid for the colloidal suspension of nanoparticles and base fluid. These nanofluids are engineered through suspension of metallic and nonmetallic particles of different shapes and sizes that are nanometer-sized or droplets in oil, water, and ethylene. When compared to traditional fluids, these nanofluids exhibit better thermophysical properties such as viscosity, thermal conductivity, and convective heat transfer coefficients [3]. In order to explain the astounding thermophysical behavior of nanofluids, Buongiorno [4] suggested seven slip mechanisms that are responsible for abnormal enhancement in thermophysical properties of nanofluids. Out of these he found that the Brownian motion and thermophoresis effects plays major role in heat transfer enhancement of nanofluids. Potential applications like energy conversion, microsystems cooling, medical industry, and optical devices and in sensors make nanofluids to be used widely. Further many researchers investigated unique heat transfer rate characteristics [5–13]. The abnormal and complex behavior of nanofluids still holds lot of mysteries, and several

CONTACT Manoj Kumar Mishra manojmishra.iitg@gmail.com Department of Mathematics, School of Advanced Sciences, VIT-AP University, Amaravati, Andhra Pradesh 522237, India.
Color versions of one or more of the figures in the article can be found online at www.tandfonline.com/unhb.

researchers are devoted to unearth the complex and abnormal thermophysical behavior of nanofluids.

Graphene is the material arranged with one atom thick layer of carbon atoms defined in hexagonal lattice, which is almost like honeycomb, pertaining to graphene outstanding properties like high elasticity, thermal conductivity, flexibility, and hardness with large resistance [14]. Graphene polymer composite is important for researchers because of its immense applications in batteries, biomedical sensors, super capacitors, and miniaturized solar or fuel cells [15]. Theoretical studies of graphene and dust particle doped magneto-Carreau fluid indicated that the combination of ethylene glycol and graphene nanoparticles improve heat transport phenomena [16]. In addition, it is reported that unsteadiness increases due to heat generation and thermal radiation, augmenting profiles of velocity and temperature [17]. Graphene based nanofluids have piqued the interest of various researchers due to its superior thermophysical, mechanical, and environmental properties.

Earlier research has primarily focused on Newtonian fluids, but many fluids used in practice are non-Newtonian, such as molten plastics and heavy oil lubricants. Additionally, dispersion of ultrafine nanoparticles into Newtonian fluids can cause them to exhibit non-Newtonian characteristics. Due to the complex nature of non-Newtonian fluids, no single equation can fully capture their properties. Further, many researchers reported beautiful complex models for non-Newtonian fluids [18–22]. All the suggested models for fluids in grades two, three, and four can evaluate the effects of elasticity but are shear independent and unable to predict shear relaxation [23]. Further the type of fluid was rated by Maxwell model which approximates shear stress relaxation. These models serve as additional evidence of the significance of boundary layer viscosity issues. In light of this, numerous scholars reported their assessments of Maxwell fluid flow problems conducted through usage of different geometrical configurations to assess various germane characteristics on the flow [24–28]. There is still dearth of research related to non-Newtonian graphene based nanofluid in the literature.

When examining industrial operations that occur at high temperatures, such as electrical power generation, furnace design, glass manufacture, missiles, and solar power technology, important properties of heat radiation for surface heat transfer cannot be overlooked. Due to depletion of traditional energy resources in the current industrial scenario, focus has been shifted to renewable energy with high sustainability. Solar energy acts as prime renewable energy source and heat radiation is significant in converting into required form depending on industrial requirements. As a result, Wang et al. [29] studies the effect of thermal radiation on non-Newtonian hydro magnetic stagnation point flow with Ohmic heating and discovered that the radiation parameter enhances the heat transfer rate. Nayak et al. [30] explained a new thermal conductivity model based on a dynamic and static method to explain the effect of heat radiation on nanofluid (Darcy–Forchheimer) flow across a rotating disk. The effect of nonlinear heat radiation on a hydromagnetic Walter-B nanofluid's stagnation point flow is discussed by Khan and Alzahrani [31], who also found that increasing the thermophoresis diffusion coefficient, thermal Biot number, and activation energy raises the temperature of the nanofluid. Abbas et al. [32] analyzed the time depended second grade fluid flow over nonlinear slandering stretching sheet under the consideration the effect of thermal radiation. Chu et al. [33] explore the effect of steady flow of Maxwell fluid due to stretching of two infinite disks with radiation is also taking into account. Varun et al. [34] analyzed the Maxwell nanofluid flow mixed with single walled carbon nanotubes(SWCNT)/ multi walled carbon nanotubes(MWCNT) considering the impact of magnetic dipole. Rasool et al. [35] explore and analyzed chemical reactive and viscous nanofluid flow *via* porous media over surface with stretching velocity. Further, many of the distinguished researchers reported new features of heat radiation on various flow fields [36–45]. Due to significant difference of temperature between free stream fluid and on the surface, many researchers analyzed the impact of heat source/sink on heat transfer nature. Keeping in view Ramzan et al. [46] explore the magnetohydrodynamic (MHD) nanofluid

(Fe_3O_4–ethylene glycol) flow over a sheet which is linearly stretched and consider the combine effect of heat generation/absorption and Cattaneo–Christov heat flux. In addition, Joule dissipation displays features such as volumetric heat source in MHD fluid flow. The combined importance of viscous and Joule dissipation is essential in perspective of the heat-treated materials. Owing to the importance of Joule dissipation, many researchers [47–50] reported the impact of Joule dissipations on fluid flow under different situations.

Present article aims to understand the impact of thermal radiation, Joule dissipation on graphene, and ethylene glycol based nanofluid flow and heat transfer across a horizontal squeezing channel by taking into account the Maxwell's non-Newtonian fluid model. The present research is motivated by following research questions:

1. How does the boundary later flow fields respond to increasing nanoparticle concentration values in a squeezing flow environment?
2. How does the Nusselt number and skin friction coefficients vary against the applied magnetic field and Joule dissipation in present flow situation?
3. What is the impact of squeezing channel over the Nusselt number and skin friction coefficients?

To the best of authors' knowledge, no investigation has been conducted on flow and heat transfer-nanofluid (ethylene glycol + graphene) passing through a squeezing channel taking into account of Joule dissipation, thermal radiation, heat absorption, and magnetic field effects. The article contains eight sections namely, Abstract, Introduction, Problem formulation, Numerical method implementation, Results and discussions, Conclusion, Acknowledgments, and References.

2. Problem formulation

The present study is formulated by taking the flow of two-dimensional (2-D) incompressible, electrically conducting, streamline, heat radiating, absorbing, and Joule dissipative Maxwell graphene nanofluid flow in squeezing channel (Figure 1). Our model is described in terms of 2-D Cartesian coordinates, in which the plates are positioned along x-axis with their normal direction along y-axis. The distance between the two plates is $h(t) = H(1-\alpha t)^{1/2}$ at time t. Now the speed and direction of plates' motion are determined by α. The plates are moving at a speed of $v(t) = \mathrm{d}h/\mathrm{d}t$, and they will ultimately meet at a time $t = 1/\ \alpha\ (\alpha \neq 0)$. If α value is negative, indicates the plates shift apart from each other. During the commencement, at the time $t = 0$, the plates

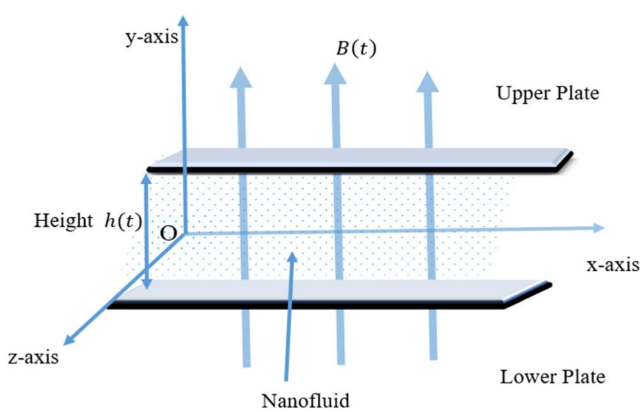

Figure 1. An illustration of the physical problem.

are separated by H. The time dependent magnetic field of strength $B(t) = B_o(1-\alpha t)^{-1/2}$ is applied in the y-direction. The mathematical model of the problem is based on following assumptions:

- It is assumed that there is no chemical reaction.
- The induced magnetic field is neglected.
- The nanoparticle and base fluid are considered to be in thermal equilibrium.
- Viscous dissipation is disregarded.

Under the above assumptions, the system of boundary layer equations representing the flow situation is given below [49]:

$$\frac{\partial u}{\partial x} + \frac{\partial v}{\partial y} = 0 \tag{1}$$

$$\frac{\partial u}{\partial t} + u\frac{\partial u}{\partial x} + v\frac{\partial u}{\partial y} = -\frac{1}{\rho_{nf}}\frac{\partial p}{\partial x} - \lambda_1\left[u^2\frac{\partial^2 u}{\partial x^2} + v^2\frac{\partial^2 u}{\partial y^2} + 2uv\frac{\partial^2 u}{\partial x \partial y}\right] - \frac{\sigma_{nf}B^2(t)\ u}{\rho_{nf}} + \vartheta_{nf}\left[\frac{\partial^2 u}{\partial x^2} + \frac{\partial^2 u}{\partial y^2}\right] \tag{2}$$

$$\frac{\partial v}{\partial t} + u\frac{\partial v}{\partial x} + v\frac{\partial v}{\partial y} = -\frac{1}{\rho_{nf}}\frac{\partial p}{\partial y} - \lambda_1\left[u^2\frac{\partial^2 v}{\partial x^2} + v^2\frac{\partial^2 v}{\partial y^2} + 2uv\frac{\partial^2 v}{\partial x \partial y}\right] + \vartheta_{nf}\left[\frac{\partial^2 v}{\partial x^2} + \frac{\partial^2 v}{\partial y^2}\right] \tag{3}$$

$$\frac{\partial T}{\partial t} + u\frac{\partial T}{\partial x} + v\frac{\partial T}{\partial y} = \frac{k_{nf}}{(\rho C_p)_{nf}}\left[\frac{\partial^2 T}{\partial x^2} + \frac{\partial^2 T}{\partial y^2}\right] + \frac{\sigma_{nf}B^2(t)u^2}{(\rho C_p)_{nf}} - \frac{1}{(\rho C_p)_{nf}}\frac{\partial q_r}{\partial y} - \frac{QT}{(\rho Cp)_{nf}} \tag{4}$$

The velocities u and v are characterized by their components in x- and y-direction and T stands for temperature. Where the relaxation time given by λ_1, fluid pressure is given as p, ρ_{nf} is the density of nanofluid, and dynamic viscosity of nanofluid is given by μ_{nf} , kinematic viscosity of nanofluid as ϑ_{nf}, the effective heat capacity of nanofluid as $(\rho C_p)_{nf}$, thermal conductivity of nanofluid as k_{nf} , the radiative heat flux of the nanofluid is given as q_r, heat absorption coefficient is given as Q, and the electrical conductivity of the nanofluid is given as σ_{nf}. The radiative heat flux is calculated using Rosseland approximation as

$$q_r = \frac{4\sigma_1}{3k_1}\frac{\partial T^4}{\partial y}$$

The Stefan–Boltzmann constant is given by σ_1, and the mean absorption coefficient is given by k_1; temperature was linearized by using Taylor series expansion of T^4 and we get

$$T^4 \cong 4T_H^3 T - 3T_H^4$$

in which the term T_H denotes the constant temperature near the wall; therefore, we attain

$$\frac{\partial q_r}{\partial y} = -\frac{16\sigma_1 T_H^3}{3k_1}\frac{\partial^2 T}{\partial y^2} \tag{5}$$

The effective nanofluid's thermophysical properties are written as follows [50]:

$$\rho_{nf} = \left[(1-\phi)\rho_f + \phi\rho_s\right] \tag{6}$$

$$(\rho C_p)_{nf} = \left[(1-\phi)(\rho C_p)_f + \phi(\rho C_p)_s\right] \tag{7}$$

$$\mu_{nf} = \frac{\mu_f}{(1-\phi)^{2.5}} \tag{8}$$

$$\frac{k_{nf}}{k_f} = \frac{k_{s+}2k_f - 2\phi(k_f - k_s)}{k_{s+}2k_f + \phi(k_f - k_s)} \tag{9}$$

$$\frac{\sigma_{nf}}{\sigma_f} = \left[1 + \frac{3\left[\frac{\sigma_s}{\sigma_f} - 1\right]\phi}{\left(\frac{\sigma_s}{\sigma_f} + 2\right) - \left(\frac{\sigma_s}{\sigma_f} - 1\right)\phi}\right] \tag{10}$$

Thermophysical properties of ethylene glycol and graphene nanoparticles are mentioned in Table 1.

The thermal conductivity of the Maxwell fluid is k_f, volume fraction of nanoparticle in nanofluid is ϕ, and thermal conductivity of solid graphene is represented by k_s. In addition, σ_s and σ_f indicate the electrical conductivity of nanoparticle and base fluid respectively. The boundary conditions are considered as follows:

$$u = 0, \ \ v = \frac{\mathrm{d}h}{\mathrm{d}t}, \ \ T = T_H \quad \text{at} \ \ y = h(t) \tag{11}$$

$$\frac{\partial u}{\partial y} = 0, \ \ v = 0, \ \ \frac{\partial T}{\partial y} = 0 \quad \text{at} \ \ y = 0 \tag{12}$$

The similarity transformation and dimensionless variables introduced are given below [51]:

$$\eta = \frac{y}{H\sqrt{1 - \alpha t}}, \quad u = \frac{\alpha x}{2(1 - \alpha t)} f'(\eta), \quad v = \frac{-\alpha H}{2\sqrt{(1 - \alpha t)}} f(\eta), \quad \theta = \frac{T}{T_H} \tag{13}$$

Following nonlinear ordinary differential equations along with thermal energy Eq. (4) are derived using dimensionless variables by removing pressure factors by cross- differentiations of Eqs. (2) and (3):

$$SA_1(1-\phi)^{2.5}\left[3f'' + \eta f''' + f'f'' - ff''' - \frac{De}{2}\left[2f'^2 f + 2f'^2 f'' - f^2 f^{iv}\right]\right] + M^2\left(\frac{\phi_b}{\phi_a}\right)f'' = f^{iv} \tag{14}$$

$$\left[1 + \frac{4}{3}R\right]\theta'' + S \cdot Pr\left(\frac{A_2}{A_3}\right)\left[f\theta' - \eta\theta'\right] + M^2\left(\frac{\phi_b}{\phi_a}\right)\frac{Pr \cdot Ec}{A_3(1-\phi)^{2.5}} f'^2 - G \cdot \theta = 0 \tag{15}$$

$$\eta = 0 \Longrightarrow f''(0) = 0, \quad f(0) = 0, \quad \theta'(0) = 0 \tag{16}$$

$$\eta = 1 \Longrightarrow f'(1) = 0, \quad f(1) = 1, \quad \theta(1) = 1 \tag{17}$$

where $S = \alpha H^2/2\vartheta_f$ indicates squeezing number, $A_1 = \rho_{nf}/\rho_f$, $A_2 = (\rho C_p)_{nf}/(\rho C_p)_f$, $A_3 = k_{nf}\ /k_f$, $\phi_a = \mu_{nf}/\mu_f$, $\phi_b = \sigma_{nf}/\sigma_f$. The Prandtl number $Pr = \mu_f(\rho C_p)_f/\rho_f k_f$, the Eckert number $Ec = (\rho_f/(\rho C_p)_f T_H)\left(\alpha x/2(1-\alpha t)\right)^2$, the Deborah number $De = \alpha\lambda_1/(1-\alpha t)$, the magnetic number $M = HB_0\sqrt{\sigma_f/\mu_f}$, $G = QH^2/k_{nf}$, and the thermal radiation parameter $R = 4\sigma_1 T_H^3/K_1\ \ k_{nf}$.

Table 1. Thermophysical properties of ethylene glycol and graphene nanoparticles [50].

Thermophysical properties	ρ (kg/m^3)	C_p (J/kg K)	k (W/mK)	σ (S/m)
Ethylene glycol	1,114	2,415	0.252	5.5×10^{-6}
Graphene	2,250	2,100	2,500	1×10^{-7}

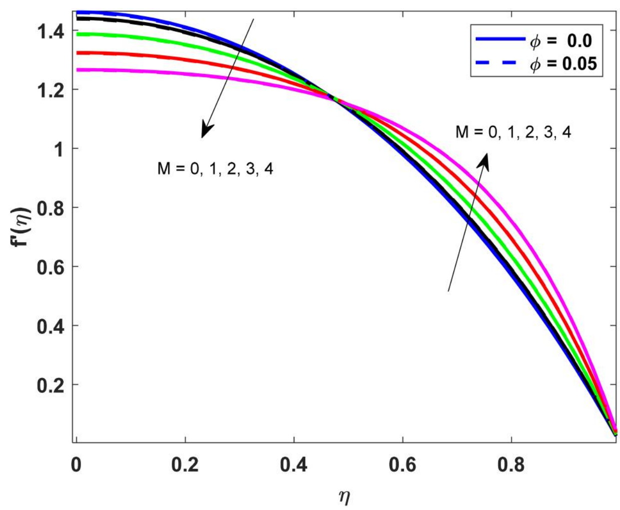

Figure 2. Velocity profiles against *M*.

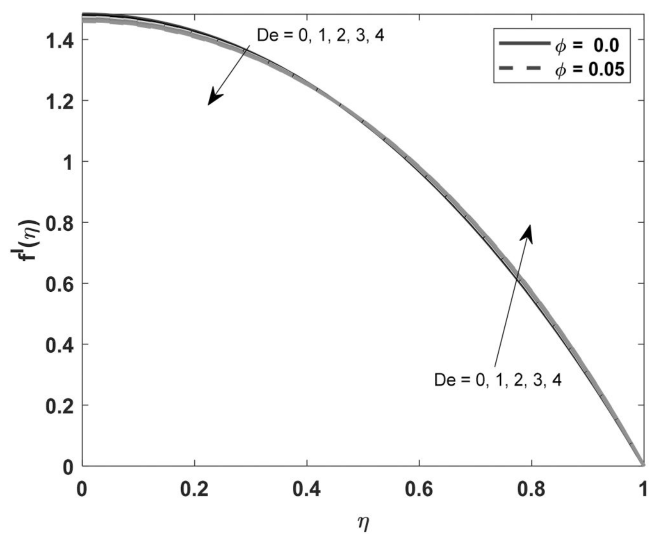

Figure 3. Velocity profiles against *De*.

The Nusselt number Nu and the coefficient of skin friction C_f can be represented as

$$C_f = \frac{\mu_{nf}\left(\frac{\partial u}{\partial y}\right)_{y=h(t)}}{\frac{1}{2}\rho_{nf}\left(\frac{dh}{dt}\right)^2} = \frac{2\ddot{f}(1)}{S\delta A_1\ (1-\phi)^{2.5}} \tag{18}$$

$$Nu = \frac{-HK_{nf}\left(\frac{\partial T}{\partial y}\right)_{y=h(t)}}{K_f\ T_H} = \frac{-Nu_r}{\sqrt{(1-\alpha t)}} \tag{19}$$

where $Nu_r = -A_3\theta'(1)$ and $\delta = H\sqrt{(1-\alpha t)}/x$.

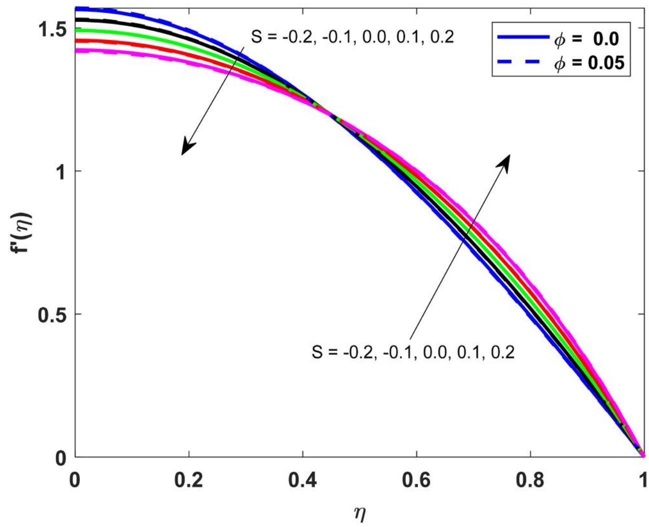

Figure 4. Velocity profiles against *S*.

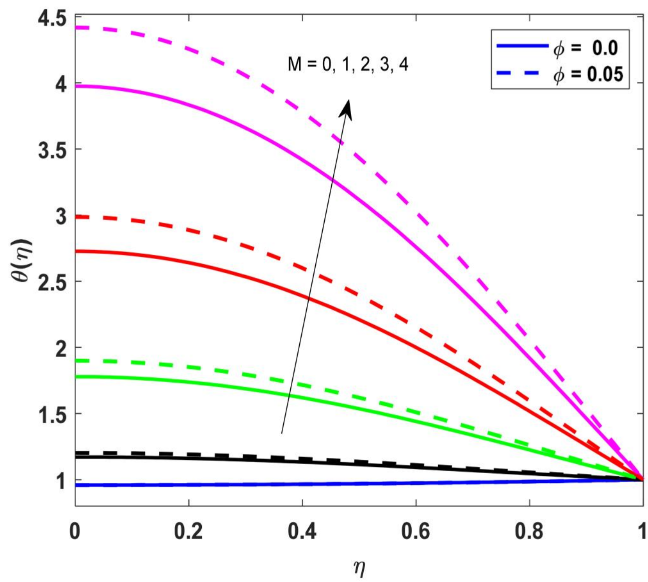

Figure 5. Temperature profiles against *M*.

3. Numerical method implementation

Because of nonlinear and coupled nature of the mathematical model, analytical solution is difficult to obtain. Thus, to find the solution of the set of nonlinear ordinary differential Eqs. (14) and (15) along with boundary conditions (16) and (17), a fourth order Runge–Kutta Fehlberg scheme along with the shooting technique is employed. At first, Eqs. (14) and (15) are converted into a set of six first order differential equations. Furthermore, to get the solution of this set of six differential equations in which initial values of functions $f''(0)$, $f'''(0)$, and $\theta'(0)$ are obtained by using of shooting technique. The step-size is chosen as 0.001 during the whole computation. To get precise result the tolerance error is selected as 10^{-6}. This whole procedure is repeated till the required accuracy in the result is attained.

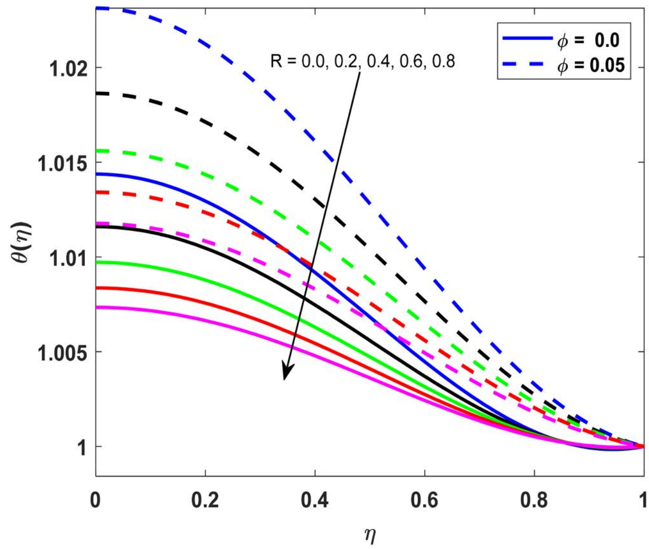

Figure 6. Temperature profiles against *R*.

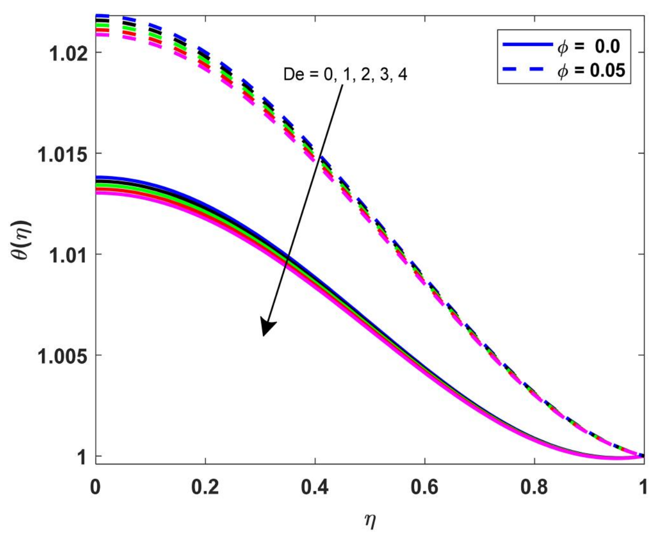

Figure 7. Temperature profiles against *De*.

4. Results and discussions

In this section, findings are represented by graphs and tabular forms. For this purpose, throughout the numerical computations, values of different types of nondimensional parameter are taken as magnetic parameter $M = 2$, Prandtl number $Pr = 11$, Eckert number $Ec = 0.05$, nanoparticle volume fraction $\phi = 0.05$, squeezing number $S = 0.1$, radiation parameter $R = 0.4$, absorption parameter $G = 0.2$, Deborah number $De = 3$, $A_1 = 0.1$, $A_2 = 0.1$, $A_3 = 0.1$. These values did not vary throughout the computation.

Figures 2–4 show the nature of the velocity along y-direction of Maxwell graphene nanofluid according to varying magnetic field, Deborah number, and squeeze number. Figure 2 presents the nature of changes of velocity along the y-direction according to change in magnetic field. It shows that if magnetic field is increasing the velocity of Maxwell graphene nanofluid is decreasing

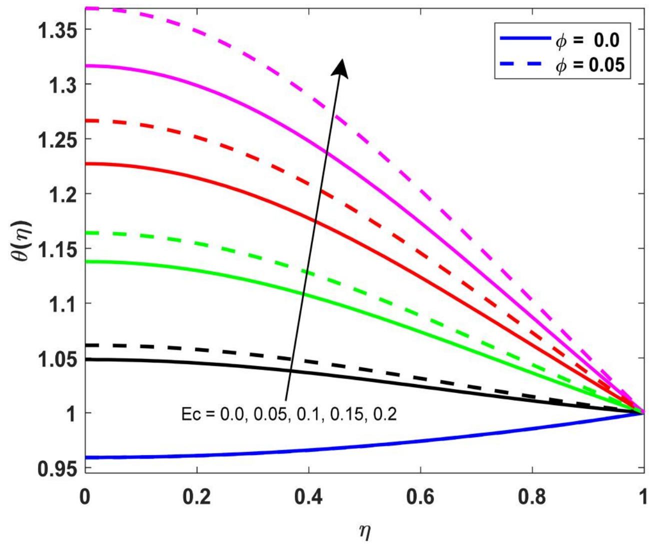

Figure 8. Temperature profiles against *Ec*.

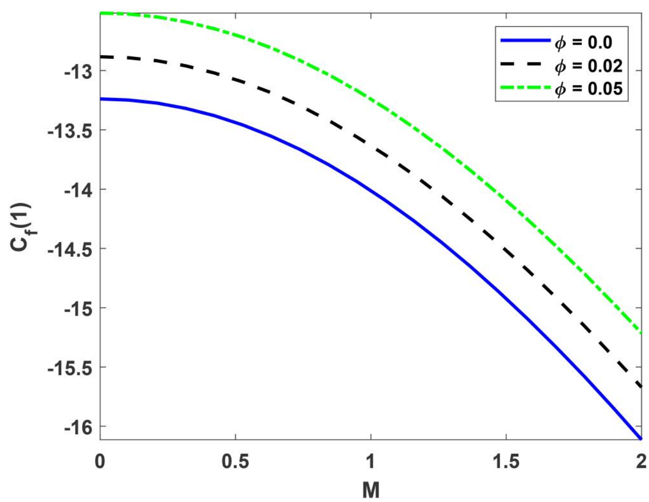

Figure 9. Skin friction coefficient C_f profiles against *M*.

up to central region whereas opposite behavior is visible after that. The reason behind this behavior of Maxwell graphene nanofluid motion up to central region is because of Lorentz force within the channel, and opposite behavior is justified by continuity equation. Figure 3 explores the effect of Deborah number in Maxwell graphene nanofluid motion. It is noted that as Deborah number increases the fluid motion decreases up to central region while opposite trends happened after central region. The logic behind this nature of the velocity up to central region is that at larger Deborah numbers, the material nature varies to increasingly dominated by elasticity (or solid like behavior). Therefore, flow velocity is going down due to increase in Deborah number. Figure 4 explores the effect of Squeeze number. It shows that as squeeze number increases the fluid motion decreases but opposite behavior seems away from the sheet.

It is clearly revealed from Figure 5 that on increasing magnetic field there is an enhancement in Maxwell graphene nanofluid temperature. The reason behind the nature of temperature of the

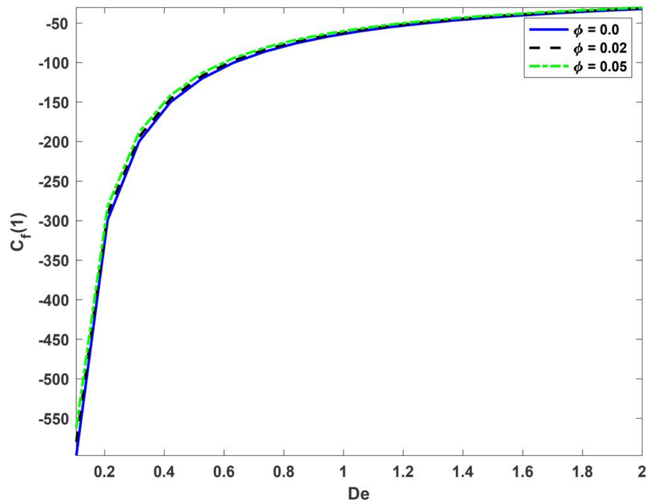

Figure 10. Skin friction coefficient C_f profiles against De.

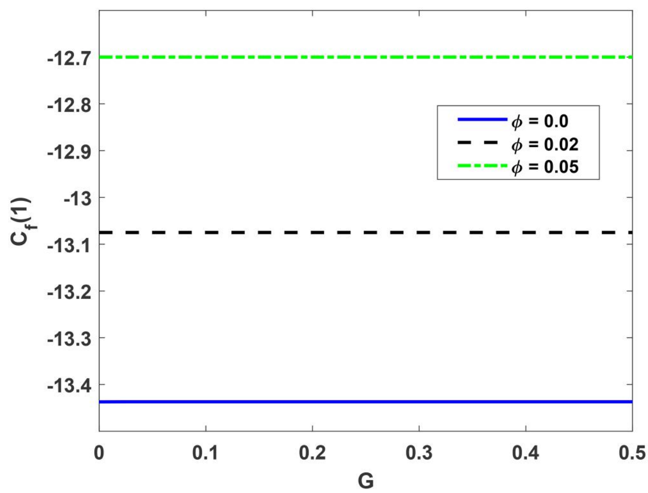

Figure 11. Skin friction coefficient C_f profiles against G.

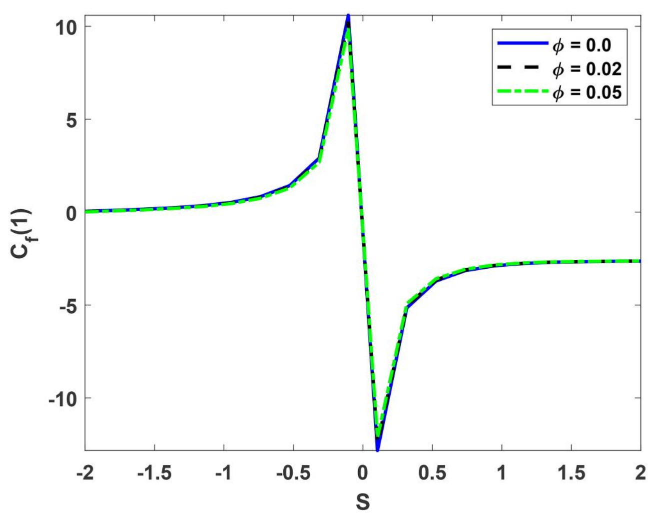

Figure 12. Skin friction coefficient C_f profiles against S.

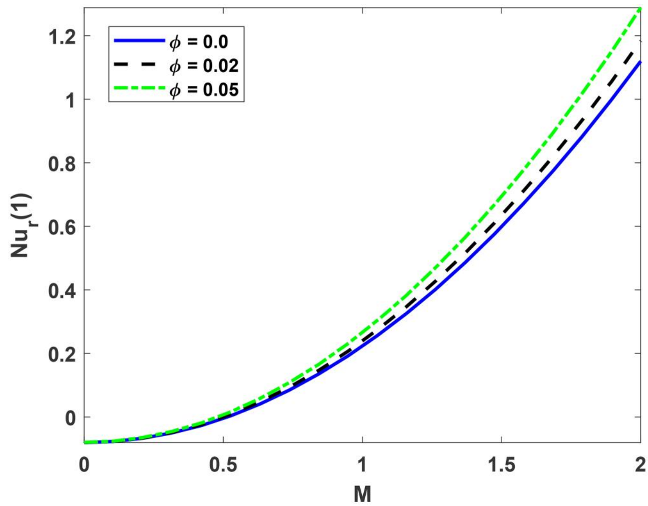

Figure 13. Nusselt number Nu_r profiles against *M*.

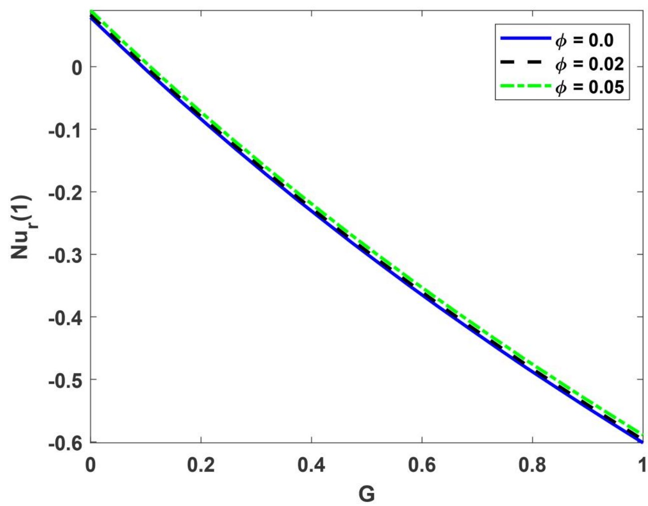

Figure 14. Nusselt number Nu_r profiles against *G*.

fluid is that as magnetic field is increasing fluid has to work more for flowing. This work is converting into the kinetic energy. Therefore, temperature is increasing.

It is depicted from Figure 6 that Maxwell graphene nanofluid temperature is reducing on increasing of radiation parameter. This happened because higher values of radiation parameter are the cause of increasing the dominating nature of conduction over radiation. Therefore, thermal boundary layer thickness is getting down and as a result heat loss is increasing.

Figure 7 depicts that Maxwell graphene nanofluid temperature is decreasing as Deborah number is increasing. Figure 8 exhibits that raising the Eckert number will also raise the temperature of the Maxwell graphene nanofluid. The theory underlying this property of Maxwell graphene nanofluid is that since the complete work is done against the viscosity and Eckert number is the ratio of kinetic energy to enthalpy, the partial kinetic energy is converting into internal energy. As a result, in the entire boundary layer domain, Joule dissipation can raise the temperature of the Maxwell graphene nanofluid.

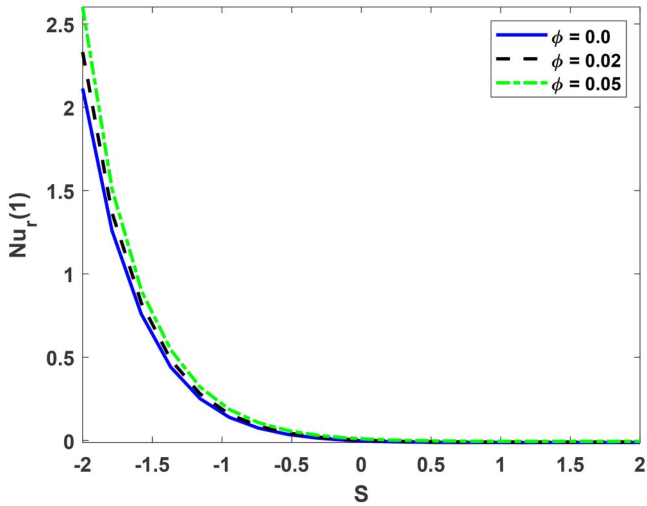

Figure 15. Nusselt number Nu_r profiles against M.

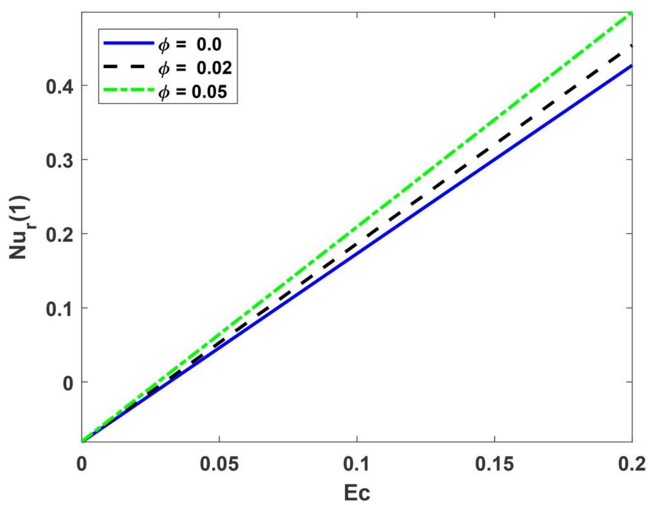

Figure 16. Nusselt number Nu_r profiles against Ec.

The values of C_f at the upper plate of the channel are computed and are displayed graphically for M, De, G, and S in Figures 9–12. An observation to Figure 9 reveals that C_f decreases when M increases.

Figures 10–12 exhibit that C_f is increasing as De, G, and S are increasing. From Figures 9–11 it is also notated that C_f is increasing as ϕ is increasing. Figure 12 shows that whenever $S < 0$, C_f decreases as ϕ increases. While for $S > 0$, C_f increases as ϕ increases.

The values of Nu are computed at the upper plate of the channel and are displayed graphically in Figures 13–16 for the M, G, S, and Ec. It is observed from Figures 13 and 16 that Nu inceases with increasing M and Ec. Figures 14 and 15 present that Nu decreases as G and S increase; it is also notated that Nu increases as ϕ increases.

It is revealed from Table 2 that the present results of this article are in excellent conformity with the result obtained in [52–54].

Table 2. Validation of $-\theta'(1)$ when $S = 0.5,\ R = 0,\ G = 0,$ and $M = 0$.

Pr	*Ec*	$-\theta'(1)$ Ref. [52]	$-\theta'(1)$ Ref. [53]	$-\theta'(1)$ Ref. [54]	$-\theta'(1)$ Present work
0.5	1.0	1.5222368	1.518 859607	1.5222367498	1.52248
1.0	1.0	3.0263240	3.019545607	3.0263235590	3.02652
2.0	1.0	5.9805300	5.967887511	5.9805303980	5.98026
5.0	1.0	14.34394100	14.413946780	14.4394132400	14.43973
1.0	0.5	1.5131620	1.509772831	1.5131618070	1.51318
1.0	1.2	3.6315880	3.623454726	3.6315882690	3.63184
1.0	2.0	6.0526470	6.039091204	6.0526471080	6.05256
1.0	5.0	15.1316200	15.097728080	15.1316178400	15.13154

5. Conclusion

The article explores the comparative study of flow and heat transfer characteristics of non-Newtonian graphene + ethylene glycol based nanofluid and simple base fluid passing through a squeezing channel under the influence of magnetic field, radiation, nanoparticle volume fraction, Joule dissipation, and Deborah number. The study carried out under the assumption that fluid is non-Newtonian and incompressible, the base fluid and nanoparticles have no chemical reaction in between, the induced magnetic field is small and neglected, nanoparticle and base fluid are considered to be in thermal equilibrium, and viscous dissipation is disregarded.

Some important findings of this study are as follows:

- The Maxwell graphene nanofluid velocity reduced due to enhancement in magnetic field, Deborah number, and squeezing number up to central region while opposite trends follow central region.
- The temperature of Maxwell graphene nanofluid is enhanced due to increasing magnetic field nanoparticle volume fraction and Joule dissipation; on the other way, opposite nature of fluid temperature is happened due to increasing radiation parameter and Deborah number.
- The local skin friction is reduced due to increase in magnetic field while opposite trends follow the Deborah number and absorption coefficient, and it also increases on increasing nanoparticle volume fraction. It is also observed that local skin friction is enhanced due to enhancing squeezing number (when $S > 0$) and reduced due to enhancing squeezing number (when $S < 0$)
- The Nusselt number is enhanced because of increasing magnetic field and Eckert number while opposite trends follow due to increasing absorption coefficient and squeezing number and it also increases on increasing nanoparticle volume fraction.
- As reported by earlier studies the graphene + ethylene glycol based nanofluid has better heat transfer characteristics compared to that of simple ethylene glycol fluid.
- It is also noted that the graphene + ethylene glycol based nanofluid displays lesser surface drag force compared to the simple base fluid (ethylene glycol).

The present research can be extended into multifaced, to name a few, it can be extended by including the entropy analysis of the present system; further in order to have improved heat transfer characteristics of the present flow system, one can consider a hybrid nanofluid flow under present physical and geometrical conditions.

Acknowledgments

The authors are warmly thankful to the reviewers for their useful comments and suggestions to improve the quality of article.

Disclosure statement

All authors agree on the submission and publication of the submitted article. The authors declare that they have no known competing financial interests or personal relationships that could have appeared to influence the work reported in this article.

ORCID

Rohit Sharma http://orcid.org/0000-0003-1885-4621
Vatukuru Nagaradhika http://orcid.org/0000-0002-0927-7191

References

[1] H. Masuda, A. Ebata, K. Teramae, and N. Hishinuma, "Alteration of thermal conductivity and viscosity of liquid by dispersing ultra-fine particles: dispersion of Al_2O_3, SiO_2 and TiO_2 ultra-fine particles," *Netsu Bussei*, vol. 7, no. 4, pp. 227–233, 1993. DOI: 10.2963/jjtp.7.227.

[2] S. U. S. Choi, "Enhancing thermal conductivity of fluids with nanoparticles," in *Developments and Applications of Non-Newtonian Flows*, vol. 66, D. A. Siginer and H. P. Wang, Eds. New York: ASME, 1995, pp. 99–105.

[3] J. A. Eastman, S. U. S. Choi, S. Li, W. Yu, and L. J. Thompson, "Anomalously increased effective thermal conductivity of ethylene glycol-based nanofluids containing copper nanoparticles," *Appl. Phys. Lett.*, vol. 78, no. 6, pp. 718–720, 2001. DOI: 10.1063/1.1341218.

[4] J. Buongiorno, "Convective transport in nanofluids," *J. Heat Transf.*, vol. 128, no. 3, pp. 240–250, 2006. DOI: 10.1115/1.2150834.

[5] L. A. Lund *et al.*, "Temporal stability analysis of magnetized hybrid nanofluid propagating through an unsteady shrinking sheet: partial slip conditions," *Comput. Mater. Contin.*, vol. 66, no. 2, pp. 1963–1975, 2021. DOI: 10.32604/cmc.2020.011976.

[6] M. Ibrahim *et al.*, "Two-phase analysis of heat transfer and entropy generation of water-based magnetite nanofluid flow in a circular microtube with twisted porous blocks under a uniform magnetic field," *Powder Technol.*, vol. 384, pp. 522–541, 2021. DOI: 10.1016/j.powtec.2021.01.077.

[7] M. Izadi, M. Ghalambaz, and S. A. M. Mehryan, "Location impact of a pair of magnetic sources on melting of a magneto-ferro phase change substance," *Chin. J. Phys.*, vol. 65, pp. 377–388, 2020. DOI: 10.1016/j.cjph.2020.03.002.

[8] A. Hajjar, S. A. M. Mehryan, and M. Ghalambaz, "Time periodic natural convection heat transfer in a nano-encapsulated phase-change suspension," *Int. J. Mech. Sci.*, vol. 166, p. 105243, 2020. DOI: 10.1016/j.ijmecsci.2019.105243.

[9] A. I. Alsabery *et al.*, "Entropy generation and natural convection flow of hybrid nanofluids in a partially divided wavy cavity including solid blocks," *Energies*, vol. 13, no. 11, p. 2942, 2020. DOI: 10.3390/en13112942.

[10] M. K. Mishra, G. S. Seth, and R. Sharma, "Scrutiny of heat transfer and nanoparticle migration within a channel filled with nanofluid," *Heat Transf.*, vol. 49, no. 5, pp. 2770–2788, 2020. DOI: 10.1002/htj.21744.

[11] U. Khan *et al.*, "γ-Nanofluid thermal transport between parallel plates suspended by micro-cantilever sensor by incorporating the effective Prandtl model: applications to biological and medical sciences,"*Molecules*, vol. 25, no. 8, p. 1777, 2020. DOI: 10.3390/molecules25081777.

[12] P. Chandra and R. Das, "Finite-element-based machine-learning algorithm for studying gyrotactic-nanofluid flow via stretching surface," *Int. J. Numer. Methods Fluids*, vol. 95, no. 12, pp. 1888–1912, 2023. DOI: 10.1002/fld.5229.

[13] I. S. Oyelakin, O. Adeyeye, P. Sibanda, and Z. Omar, "On a new block method for an MHD nanofluid flow with an exponentially decaying internal heat generation," *Numer. Methods Fluids*, vol. 93, no. 6, pp. 1816–1824, 2021. DOI: 10.1002/fld.4953.

[14] A. H. Castro Neto, F. Guinea, N. M. R. Peres, K. S. Novoselov, and A. K. Geim, "The electronic properties of graphene," *Rev. Mod. Phys*, vol. 81, no. 1, pp. 109–162, 2009. DOI: 10.1103/RevModPhys.81.109.

[15] C. Chung *et al.*, "Biomedical applications of graphene and graphene oxide," *Acc. Chem. Res.*, vol. 46, no. 10, pp. 2211–2224, 2013. DOI: 10.1021/ar300159f.

[16] S. M. Upadhya, Mahesha, and C. S. K. Raju, "Unsteady flow of Carreau fluid in a suspension of dust and graphene nanoparticles with Cattaneo–Christov heat flux," *J. Heat Transf.*, vol. 140, no. 9, p. 092401, 2018. DOI: 10.1115/1.4039904.

[17] Mahesha, H. B. Santhosh, and C. S. K. Raju, "Unsteady Carreau radiated flow in a deformation of graphene nanoparticles with heat generation and convective conditions," *J. Nanofluids*, vol. 7, no. 6, pp. 1130–1137, 2018. DOI: 10.1166/jon.2018.1545.

[18] S. Barış and M. S. Dokuz, "Three-dimensional stagnation point flow of a second-grade fluid towards a moving plate," *Int. J. Eng. Sci*, vol. 44, no. 1–2, pp. 49–58, 2006. DOI: 10.1016/j.ijengsci.2005.08.008.

[19] M. H. Haroun, "Effect of Deborah number and phase difference on peristaltic transport of a third-order fluid in an asymmetric channel," *Commun. Nonlinear Sci. Numer. Simul.*, vol. 12, no. 8, pp. 1464–1480, 2007. DOI: 10.1016/j.cnsns.2006.03.002.

[20] M. Sajid, T. Hayat, and S. Asghar, "Non-similar analytic solution for MHD flow and heat transfer in a third-order fluid over a stretching sheet," "*Int. J. Heat Mass Transf.*, vol. 50, no. 9–10, pp. 1723–1736, 2007. DOI: 10.1016/j.ijheatmasstransfer.2006.10.011.

[21] T. Hayat, S. Noreen, and M. Sajid, "Heat transfer analysis of the steady flow of a fourth grade fluid," *Int. J. Therm. Sci.*, vol. 47, no. 5, pp. 591–599, 2008. DOI: 10.1016/j.ijthermalsci.2007.05.005.

[22] Y.-M. Chu *et al.*, "Cattaneo-Christov double diffusions (CCDD) in entropy optimized magnetized second grade nanofluid with variable thermal conductivity and mass diffusivity," *J. Mater. Res. Technol.*, vol. 9, no. 6, pp. 13977–13987, 2020. DOI: 10.1016/j.jmrt.2020.09.101.

[23] T. Hayat, A. M. Siddiqui, and S. Asghar, "Some simple flows of an Oldroyd-B fluid," *Int. J. Eng. Sci.*, vol. 39, no. 2, pp. 135–147, 2001. DOI: 10.1016/S0020-7225(00)00026-4.

[24] C. Fetecau and C. Fetecau, "A new exact solution for the flow of Maxwell fluid past an infinite plate," *Int. J. Non-Linear Mech.*, vol. 38, no. 3, pp. 423–427, 2003. DOI: 10.1016/S0020-7462(01)00062-2.

[25] Y. Wang and T. Hayat, "Fluctuating flow of Maxwell fluid past a porous plate with variable suction," *Nonlinear Anal. Real World Appl.*, vol. 9, no. 4, pp. 1269–1282, 2008. DOI: 10.1016/j.nonrwa.2007.02.016.

[26] C. Fetecau, M. Athar, and C. Fetecau, "Unsteady flow of a generalized Maxwell fluid with fractional derivative due to a constantly accelerating plate," *Comput. Math. Appl.*, vol. 57, no. 4, pp. 596–603, 2009. DOI: 10.1016/j.camwa.2008.09.052.

[27] T. Hayat, Z. Abbas, and M. Sajid, "MHD stagnation point flow of an upper-convected Maxwell fluid over a stretching surface," *Chaos Solit. Fractals*, vol. 39, no. 2, pp. 840–848, 2009. DOI: 10.1016/j.chaos.2007.01.067.

[28] M. M. Heyhat and N. Khabazi, "Non-isothermal flow of Maxwell fluids above fixed flat plates under the influence of a transverse magnetic field," *Proc. Inst. Mech. Eng. C: J. Mech. Eng. Sci.*, vol. 225, no. 4, pp. 909–916, 2011. DOI: 10.1243/09544062JMES2245.

[29] J. Wang, M. Ijaz Khan, W. A. Khan, S. Z. Abbas, and M. Imran Khan, "Transportation of heat generation/absorption and radiative heat flux in homogeneous–heterogeneous catalytic reactions of non-Newtonian fluid (Oldroyd-B model)," *Comput. Methods Programs Biomed.*, vol. 189, p. 105310, 2020. DOI: 10.1016/j.cmpb.2019.105310.

[30] M. K. Nayak, S. Shaw, M. I. Khan, V. S. Pandey, and M. Nazeer, "Flow and thermal analysis on Darcy-Forchheimer flow of copper-water nanofluid due to a rotating disk a static and dynamic approach," *J. Mater. Res. Technol.*, vol. 9, no. 4, pp. 7387–7408, 2020. DOI: 10.1016/j.jmrt.2020.04.074.

[31] M. I. Khan and F. Alzahrani, "Activation energy and binary chemical reaction effect in nonlinear thermal radiative stagnation point flow of Walter-B nanofluid: numerical computations," *Int. J. Mod. Phys. B*, vol. 34, no. 13, p. 2050132, 2020. DOI: 10.1142/S0217979220501325.

[32] S. Z. Abbas *et al.*, "Modeling and analysis of unsteady second-grade nanofluid flow subject to mixed convection and thermal radiation," *Soft Comput.*, vol. 26, no. 3, pp. 1033–1042, 2022. DOI: 10.1007/s00500-021-06575-7.

[33] Y.-M. Chu *et al.*, "Thermophoretic particles deposition features in thermally developed flow of Maxwell fluid between two infinite stretched disks," *J. Mater. Res. Technol.*, vol. 9, no. 6, pp. 12889–12898, 2020. DOI: 10.1016/j.jmrt.2020.09.011.

[34] V. Kumar *et al.*, "Analysis of single and multi-wall carbon nanotubes (SWCNT/MWCNT) in the flow of Maxwell nanofluid with the impact of magnetic dipole," *Comput. Theor. Chem.*, vol. 1200, p. 113223, 2021. DOI: 10.1016/j.comptc.2021.113223.

[35] G. Rasool, A. Shafiq, Y. M. Chu, M. S. Bhutta, and A. Ali, "Optimal homotopic exploration of features of Cattaneo-Christov model in second grade nanofluid flow via Darcy-Forchheimer medium subject to viscous dissipation and thermal radiation," *Comb. Chem. High Throughput Screen.*, vol. 25, no. 14, pp. 2485–2497, 2022. DOI: 10.2174/1386207324666210903144447.

[36] S. Vemulawada *et al.*, "Thermal analysis on electromagnetic regulated peristaltic blood-based graphane/diamond nanofluid flow with entropy optimization," *Numer. Heat Transf. B: Fundam.*, vol. 84, no. 5, pp. 514–538, 2023. DOI: 10.1080/10407790.2023.2211731.

[37] X. Xue and H. Zhou, "Soft computing methods for predicting daily global solar radiation," *Numer. Heat Transf. B: Fundam.*, vol. 76, no. 1, pp. 18–31, 2019. DOI: 10.1080/10407790.2019.1637629.

[38] D.-S. Yang, *et al.*, "Calculating the multi-domain transient heat conduction with heat source problem by virtual boundary meshfree Galerkin method," *Numer. Heat Transf. B: Fundam.*, vol. 74, no. 1, pp. 465–479, 2018. DOI: 10.1080/10407790.2018.1505091.

[39] M. K. Mishra, G. S. Seth, and R. Sharma, "Navier's slip effect on mixed convection flow of non-Newtonian nanofluid: Buongiorno's model with passive control approach," *Int. J. Appl. Comput. Math.*, vol. 5, no. 4, pp. 1–23, 2019. DOI:10.1007/s40819-019-0686-z.

[40] A. Ghaffari, I. Mustafa, and T. Javed, "Influence of nonlinear radiation on natural convection flow of carbon nanotubes suspended in water-based fluid along a vertical wavy surface," *Phys. Scr.*, vol. 94, no. 11, p. 115214, 2019. DOI: 10.1088/1402-4896/ab23b8.

[41] M. Shahzad *et al.*, "Transport of radiative heat transfer in dissipative cross nanofluid flow with entropy generation and activation energy," *Phys. Scr.*, vol. 94, no. 11, p. 115224, 2019. DOI: 10.1088/1402-4896/ab2caf.

[42] H. Waqas, S. U. Khan, M. Imran, and M. M. Bhatti, "Thermally developed Falkner–Skan bioconvection flow of a magnetized nanofluid in the presence of a motile gyrotactic microorganism: buongiorno's nanofluid model," *Phys. Scr.*, vol. 94, no. 11, p. 115304, 2019. DOI: 10.1088/1402-4896/ab2ddc.

[43] E. Hosseini, G. B. Loghmani, M. Heydari, and M. M. Rashidi, "A numerical simulation of MHD flow and radiation heat transfer of nanofluids through a porous medium with variable surface heat flux and chemical reaction," *J. Math. Ext.*, vol. 13, pp. 31–67, 2019.

[44] K. Ramesh *et al.*, "Bioconvection assessment in Maxwell nanofluid configured by a Riga surface with nonlinear thermal radiation and activation energy," *Surf. Interfaces*, vol. 21, p. 100749, 2020. DOI: 10.1016/j.surfin.2020.100749.

[45] S. Muthukumar, S. Sureshkumar, S. El-Sapa, and A. J. Chamkha, "Impacts of uniform and sinusoidal heating in a nanofluid saturated porous chamber influenced by the thermal radiation and the magnetic field," *Numer. Heat Transf. A: Appl.*, vol. 84, no. 5, pp. 488–506, 2023. DOI: 10.1080/10407782.2022.2137072.

[46] M. Ramzan, N. Shaheen, H. A. S. Ghazwani, Y. Elmasry, and S. Kadry, "Application of Corcione correlation in a nanofluid flow on a bidirectional stretching surface with Cattaneo–Christov heat flux and heat generation/absorption," *Numer. Heat Transf. A: Appl.*, vol. 84, no. 6, pp. 569–585, 2023. DOI: 10.1080/10407782.2022.2145396.

[47] S. P. Anjali Devi and B. Ganga, "Effects of viscous and Joules dissipation on MHD flow, heat and mass transfer past a stretching porous surface embedded in a porous medium," *Nonlinear Anal. Model. Control*, vol. 14, no. 3, pp. 303–314, 2009. DOI: 10.15388/NA.2009.14.3.14497.

[48] Y. S. Daniel, Z. A. Aziz, Z. Ismail, and F. Salah, "Effects of thermal radiation, viscous and Joule heating on electrical MHD nanofluid with double stratification," *Chin. J. Phys.*, vol. 55, no. 3, pp. 630–651, 2017. DOI: 10.1016/j.cjph.2017.04.001.

[49] R. Sharma, S. M. Hussain, C. S. K. Raju, G. S. Seth, and A. J. Chamakha, "Study of graphene Maxwell nanofluid flow past a linearly stretched sheet: a numerical and statistical approach," *Chin. J. Phys.*, vol. 68, pp. 671–683, 2020. DOI: 10.1016/j.cjph.2020.10.013.

[50] S. M. Hussain, R. Sharma, M. R. Mishra, and S. S. Alrashidy, "Hydromagnetic dissipative and radiative graphene Maxwell nanofluid flow past a stretched sheet-numerical and statistical analysis," *Mathematics*, vol. 8, no. 11, p. 1929, 2020. DOI: 10.3390/math8111929.

[51] G. C. Shit and S. Mukherjee, "Differential transform method for unsteady magneto hydrodynamic nanofluid flow in the presence of thermal radiation," *J. Nanofluids*, vol. 8, no. 5, pp. 998–1009, 2019. DOI: 10.1166/jon.2019.1643.

[52] M. Mustafa, T. Hayat, and S. Obaidat, "On heat and mass transfer in the unsteady squeezing flow between parallel plates," *Meccanica*, vol. 47, no. 7, pp. 1581–1589, 2012. DOI: 10.1007/s11012-012-9536-3.

[53] O. Pourmehran, M. Rahimi-Gorji, M. Gorji-Bandpy, and D. Ganji, "Analytical investigation of squeezing unsteady nanofluid flow between parallel plates by LSM and CM," *Alex. Eng. J.*, vol. 54, no. 1, pp. 17–26, 2015. DOI: 10.1016/j.aej.2014.11.002.

[54] N. Acharya, K. Das, and P. K. Kundu, "The squeezing flow of Cu-water and Cu-kerosene nanofluids between two parallel plates," *Alex. Eng. J.*, vol. 55, no. 2, pp. 1177–1186, 2016. DOI: 10.1016/j.aej.2016.03.039.